RSC Advances

PAPER

View Article Online
View Journal | View Issue

Cite this: *RSC Adv.*, 2017, **7**, 16149

Dimetallofullerene $M_2@C_{100}$ or carbide cluster fullerene $M_2C_2@C_{98}$ (M = La, Y, and Sc): which ones are more stable?†

Lei Mu,[a] Xiaodi Bao,[a] Shumei Yang[a] and Xianglei Kong*[ab]

Received 17th January 2017
Accepted 1st March 2017

DOI: 10.1039/c7ra00717e

rsc.li/rsc-advances

The geometric and thermodynamic stability of the M_2C_{100} (M = La, Y, and Sc) series was systematically investigated using density functional theory calculations on the level of B3LYP/6-31G(d) ~ Lanl2dz. In all the cases, $M_2@D_5(285913)$-C_{100} isomers are the lowest-energy species. However, carbide endohedral fullerenes $M_2C_2@C_1(230933)$-C_{98} present excellent thermodynamic stabilities, except for those with La metal. The main product in electric arc experiments at temperatures lower than 3500 K for La_2C_{100} should be $La_2@D_5(285913)$-C_{100}, which was successfully synthesized previously; for Y and Sc, the predicted main products in these experiments should be $M_2C_2@C_1(230933)$-C_{98}. Further analysis of the geometric structures of the M_2C_{100} series showed that the dimetallofullerenes $M_2@C_{100}$ have greater effects on the shapes of cages than $M_2C_2@C_{98}$. These results provide some valuable guidance for the synthesis and characterization of large endohedral fullerenes including La, Y or Sc.

Introduction

Endohedral dimetallofullerenes were firstly considered to exist in the form of $M_2@C_{2n}$.[1–9] However, based on ^{13}C NMR spectroscopic studies, Wang *et al.* found that the previously suggested endohedral metallofullerene (EMF) of $Sc_2@C_{86}$ was in fact, $Sc_2C_2@C_{84}$.[10] Since then, many types of carbide cluster fullerenes have been widely reported. It is well known that EMFs of M_2C_{2n} may exist in two distinguished forms: classical dimetallofullerenes, $M_2@C_{2n}$, or carbide cluster fullerenes $M_2C_2@C_{2n-2}$.[11–16] Among the reported carbide cluster fullerenes, Sc plays a very important role; for example, the reported carbide cluster fullerenes with two Sc atoms include $Sc_2C_2@C_{84}$,[8,10,17] $Sc_2C_2@C_{82}$,[12,18] $Sc_2C_2@C_{80}$ (ref. 4 and 11) and $Sc_2C_2@C_{68}$.[15] Recently, a family of $Y_2C_2@C_{2n}$ was isolated by Dorn *et al.*, and some of them were determined by ^{13}C NMR spectroscopy,[9] whereas the isolation and crystallographic characterization of $La_2C_2@C_{2n}$ is less reported.[19,20] On the other hand, many dimetallofullerenes of $M_2@C_{2n}$ have also been identified; for example, structures of $Sc_2@C_{66}$,[21] $Sc_2@C_{82}$ (ref. 22) and $Y_2@C_{82}$ (ref. 23) have been determined by ^{13}C NMR spectroscopy. Dimetallofullerenes of $La_2@C_{2n}$ including $La_2@C_{72}$,[24] $La_2@C_{78}$ (ref. 25) and $La_2@C_{80}$ (ref. 26) have also been synthesized and characterized.

Recently, endohedral fullerenes with large cage sizes ($n > 90$) have attracted significant research interest;[27–30] for example, the largest fullerene cage that has been identified by X-ray is $Sm_2@D_{3d}(822)$-C_{104}, which shows a nanotubular shape,[27] and a series of EMFs containing two gadolinium atoms with cages from C_{90} to C_{124} have been observed by Yang *et al.*[28] However, the effective isolation and structural characterization of these EMFs are still very challenging; for example, Christine M. Beavers *et al.* discovered an extensive series of soluble dilanthanum endohedral fullerenes from La_2C_{90} to La_2C_{138}, but only a very few of them have been isolated in pure form and characterized by single-crystal X-ray diffraction.[29]

Due to the difficulty in synthesis, separation and structural assignment of these species, theoretical study has been widely performed to help to predict or determine the structure, stability and properties of these species.[31–36] There are at least two challenges in these calculations that should be mentioned. First, the number of different cage isomers for a particular cage size quickly increases with the cage size. Since the non-IPR cages can be greatly stabilized by the encaged metal atoms in EMFs, they should be considered in many cases. Yang *et al.* performed a systematic investigation on the structures of $Dy_2@C_{100}$ including IPR and non-IPR isomers (with a total number of 24 755) and found that the $D_5(285913)$-C_{100} cage was the most promising candidate for encapsulation.[31] Second, for EMFs having the form of M_2C_{2n}, both dimetallofullerenes $M_2@C_{2n}$ and carbide cluster fullerenes $M_2C_2@C_{2n-2}$ should be considered and compared. For example, in order to deduce the most stable isomers of M_2C_{98} (M = Sc, Y, La, Gd, Lu), Zheng *et al.* performed systematic studies on the series by density

[a]*The State Key Laboratory of Elemento-Organic Chemistry, College of Chemistry, Nankai University, Tianjin, 300071, China. E-mail: kongxianglei@nankai.edu.cn*
[b]*Collaborative Innovation Center of Chemical Science and Engineering, Nankai University, Tianjin 300071, China*

† Electronic supplementary information (ESI) available. See DOI: 10.1039/c7ra00717e

functional theory (DFT) methods, and found that the metal-carbide endohedral fullerenes are more stable.[34]

In order to better understand the structures of large-sized EMFs, herein, we conduct a comprehensive analysis on M_2C_{100} (M = La, Y, Sc) with DFT methods. The geometric structure and thermodynamic stability of M_2C_{100} species, including dimetallofullerenes of $M_2@C_{100}$ (based on the full screening of 285913 C_{100} cages) and carbide cluster fullerenes of $M_2C_2@C_{98}$ (based on full screening of 231017 C_{98} cages), have been systematically investigated. Interestingly, our results show that compared with the previous results of M_2C_{98} obtained by Zheng *et al.*,[34] the increase in the cage by only a single unit of C_2 does affect their energy priorities for corresponding dimetallofullerenes and carbide cluster fullerenes, implying the difficulty in predicting their structures and energies for EMFs with larger cages.

Computational details

It is known that each encapsulated metal atom of La, Y or Sc will donate three electrons to the fullerene cage in $M_2@C_{2n}$ isomers;[34–36] thus, the geometry optimization of $M_2@C_{2n}$ isomers (M = La, Y, Sc) was set based on the optimization results of C_{100}^{6-}. Since non-IPR fullerenes can be stabilized by the inside metal ions, the total of 24 755 isomers, including all 450 IPR (isolated-pentagon-rule) isomers and 24 305 non-IPR isomers with less than two adjacent pentagons, were considered here. The 5 most stable isomers of C_{100}^{6-} were taken from the previous results reported by Yang *et al.*[31] For $M_2C_2@C_{98}$ (M = La, Y, Sc), the encapsulated M_2C_2 clusters maintain a + 4 valence state and thus, their geometry optimizations were performed based on the optimization results of C_{98}^{4-}. A total of 17 941 carbon cages, including all 259 IPR and 17 232 non-IPR cages with less than two adjacent pentagons, were first calculated at the AM1 level (Table S1†). Then, the ten lowest-energy C_{98}^{4-} (Table S2†) cages and five lowest-energy C_{100}^{6-} cages were further optimized at the level of B3LYP/6-31G. After that, optimized metalloclusters M_2 (M = La, Y, Sc) or M_2C_2 (M = La, Y, Sc) were put into the corresponding C_{100}^{6-} and C_{98}^{4-} cages in different directions. All these isomers of $M_2@C_{100}$ and the six most stable isomers of $M_2C_2@C_{98}$ were at last optimized at the B3LYP/6-31G(d) ~ Lanl2dz level and further verified by vibrational analysis on the same level. For all these species, electronic energies were calculated at 0 K with zero-point energy corrections and free energies were calculated at 298 K. All DFT calculations were carried out using the Gaussian 09 program package.[37]

Relative concentrations (W_i) of the ith isomer at different temperatures were calculated using the following equation:[38]

$$W_i = \frac{q_i \exp\left(-\frac{\Delta H^{\circ}_{0,i}}{RT}\right)}{\sum_{j=1}^{n} q_j \exp\left(-\frac{\Delta H^{\circ}_{0,j}}{RT}\right)}$$

where R is the gas constant, T is the absolute temperature, q_i and $\Delta H^{\circ}_{0,i}$ are the partition function and the relative heat of formation at absolute zero temperature of the ith isomer, respectively. Chirality contributions were also taken into account by doubling their partition functions for enantiomeric pairs, and rotational–vibrational partition functions were calculated from the optimized structural and vibrational data obtained at the level of B3LYP/6-31G(d) ~ Lanl2dz without frequency scaling.

Results and discussion

Table 1 shows the relative energies and HOMO–LUMO gaps of M_2C_{100} isomers (M = La, Y, Sc) optimized at the level of B3LYP/6-31G(d) ~ Lanl2dz. All the isomers were calculated based on closed-shell electron configurations. The results show that for La, the two isomers with lowest energies are $La_2@D_5(285913)$-C_{100} and $La_2@C_2(285864)$-C_{100}, in which the latter has an energy of 17.9 kcal mol^{-1} higher than that of the former. Among the carbide cluster fullerenes, the isomer with the lowest energy is $La_2C_2@C_1(230933)$-C_{98}, which is 34.6 kcal mol^{-1} higher in

Table 1 Relative energies and HOMO–LUMO gaps of M_2C_{100} isomers (M = La, Y, and Sc)[a,b]

Spiral ID[c]	IPR ID[d]	PA[e]	Sym.[f]	ΔE^g (La)	Gap[h] (La)	ΔE^g (Y)	Gap[h] (Y)	ΔE^g (Sc)	Gap[h] (Sc)
C_{98}-230924	166	0	C_2	45.0	1.05	18.4	1.16	9.6	1.13
C_{98}-230925	167	0	C_{2v}	—	—	—	—	10.5	1.57
C_{98}-230926	168	0	C_1	45.2	1.25	17.9	1.25	8.2	1.26
C_{98}-230933	175	0	C_1	34.6	1.48	10.7	1.48	0.9	0.90
C_{98}-230979	221	0	C_2	52.0	1.50	24.0	1.36	13.9	1.38
C_{98}-230600		1	C_1	63.8	1.04	31.0	1.05	15.2	1.44
C_{100}-285793	330	0	C_2	21.8	1.08	17.0	1.19	14.4	1.41
C_{100}-285858	395	0	D_{2d}	22.8	1.26	18.6	1.34	13.9	1.61
C_{100}-285864	401	0	C_2	17.9	0.88	19.6	1.10	19.6	1.22
C_{100}-285868	405	0	C_1	26.4	0.84	20.7	0.89	14.8	1.32
C_{100}-285913	450	0	D_5	0	1.54	0	1.54	0	1.85

[a] Optimization was performed on the basis of B3LYP/6-31G(d) ~ Lanl2dz. [b] Optimization of the isomers of $M_2@C_{98}$-230925 (M = La, Y) failed. [c] Based on IUPAC standards to encode all of the carbon cages. [d] Based on IUPAC standards to encode the carbon cages abiding by IPR rules. [e] The number of adjacent pentagons. [f] Symmetry of the original empty carbon cage, which is also applied in the nomenclature of the EMFs (after the symbol of @). [g] Relative energy units in kcal mol^{-1}. [h] Units in eV.

energy than $La_2@D_5(285913)$-C_{100}. A comparison among their relative energies is also shown in Fig. S1a,† where it can be seen that the energies of the $La_2@C_{100}$ isomers are generally lower, compared to those of $La_2C_2@C_{98}$. It is also revealed in Table 1 that the isomer $La_2@D_5(285913)$-C_{100} has a considerably large HOMO–LUMO gap (1.54 eV), indicating its prominent chemical stability. For the IPR-violating fullerene of $La_2@C_1(230600)$-C_{98}, its relative energy is found to be much higher, compared to those of IPR. To further confirm the results, a different pseudopotential of ECP46MHF was also applied,[39] and the results were similar. The energy of $La_2C_2@C_1(230933)$-C_{98} is 40.2 kcal mol^{-1} higher than that of $La_2@D_5(285913)$-C_{100} and their gaps are 0.1 eV and 0.02 eV lower than the results obtained with the pseudopotential of Lanl2dz for the two species, respectively.

To evaluate the overall thermodynamic stability of these EMFs at relatively high temperatures, their temperature-relative concentration curves were calculated and are shown in Fig. 1a. All thermodynamic properties were evaluated using the harmonic approximation to calculate the partition function. Errors caused by anharmonicity are not considered here. Under temperatures lower than 2000 K, the relative concentration of $La_2@D_5(285913)$-C_{100} dominates the distribution. With increasing temperature, the concentration decreases and is surpassed by the isomer of $La_2C_2@C_1(230933)$-C_{98} at 3500 K. At about 3500 K, the relative concentration of $La_2C_2@C_1(230933)$-C_{98} ascends to 35% and prevails with the increase in temperature. As a result, dimetallofullerenes display distinct stability at low temperature, but carbide cluster fullerenes are more stable when the temperature is higher than 3500 K. The result suggests that the isomer of $La_2@D_5(285913)$-C_{100} may exist and accounts for an important component in the synthesis, which matches well with the experimental results reported by Beavers *et al.*[29] In their electric arc experiments, a series of EMFs from La_2C_{90} to La_2C_{138} was discovered, and the most abundant product was found to be $La_2@D_5(285913)$-C_{100}, which was isolated in pure form and characterized by X-ray diffraction. The consistent results also prove that our theoretical calculation results performed here are reliable and credible.

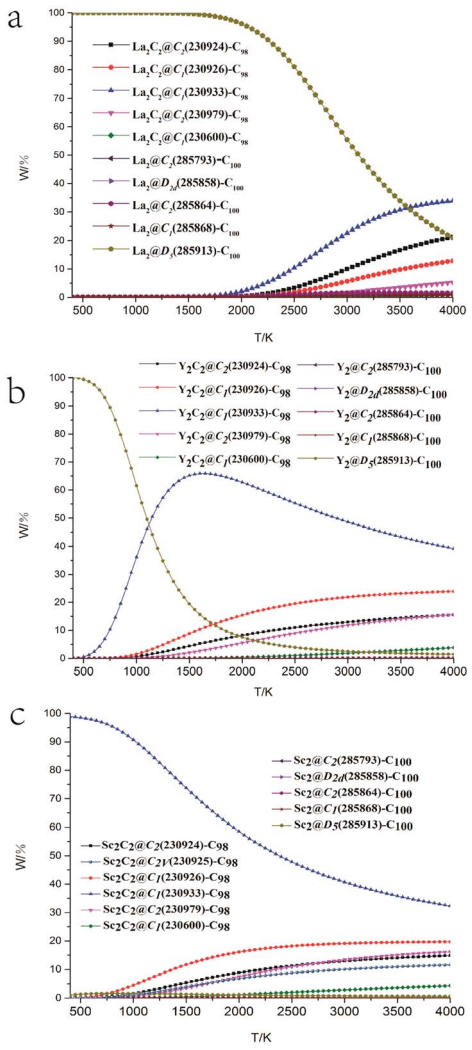

Fig. 1 Relative concentrations of low-energy isomers of (a) La_2C_{100}, (b) Y_2C_{100} and (c) Sc_2C_{100}.

Based on a similar calculation strategy, further studies with Y and Sc atoms were also carried out. These results are also shown in Table 1. $Y_2@D_5(285913)$-C_{100} and $Sc_2@D_5(285913)$-C_{100} are the lowest-energy isomers of $Y_2@C_{100}$ and $Sc_2@C_{100}$, respectively. For carbide cluster fullerenes, the isomers with the lowest energies still have the IPR cages of $C_1(230933)$-C_{98}. However, the energy differences between pure EMFs and metal carbide EMFs for different metal atoms are different. The energy of $Y_2C_2@C_1(230933)$-C_{98} was found to be 10.7 kcal mol^{-1} higher than that of $Y_2@D_5(285913)$-C_{100}, and the value decreases to 0.90 kcal mol^{-1} in the case of Sc_2C_{100}. A comparison among the relative energies of all calculated isomers of $M_2@C_{100}$ and $M_2C_2@C_{98}$ (M = Y, Sc) is shown in Table S4,† where their differences are clearly reflected. For Y_2C_{100}, the energies of $Y_2@C_{100}$ isomers and those of $Y_2C_2@C_{98}$ are very close, and they change their energy orders sequentially. However, the energies for corresponding $Sc_2C_2@C_{98}$ isomers are generally lower than those of $Sc_2@C_{100}$, except for the most stable isomer of $Sc_2@D_5(285913)$-C_{100}. Triplet states of some isomers are also considered (Table S4†) and their energies are obviously higher than those of singlet states.

Relative concentrations of M_2C_{100} (M = Y, Sc) isomers under different temperatures are shown in Fig. 1b and c, respectively. $Y_2@D_5(285913)$-C_{100}, the lowest-energy structure in the Y_2C_{100} series is prevalent under low temperature below 500 K. With temperature increasing, its relative concentration descends sharply and is surpassed by $Y_2C_2@C_1(230933)$-C_{98} at 1100 K. At about 1700 K, the relative concentration of $Y_2C_2@C_1(230933)$-C_{98} ascends to its maximum yield of 65%. Though its concentration decreases after 1700 K, it still occupied the main fraction. $Y_2C_2@C_1(230933)$-C_{98} together with the other three carbide cluster fullerenes share the largest contributions when the temperature is higher than 3500 K. For the Sc_2C_{100} system (Fig. 1c), the relative concentration of $Sc_2@D_5(285913)$-C_{100}, which is the lowest-energy structure at 0 K, can be totally neglected under general temperature. In contrast, the relative concentration of $Sc_2C_2@C_1(230933)$-C_{98} decreases to about 55% at 2000 K and keeping declining with increasing temperature, but is still significantly higher than other isomers. Like the

Y_2C_{100} system, carbide cluster fullerene isomers are dominant in the high temperature region. The results reflect a similar trend to the M_2C_{98} (M = Y, Sc) series, in which M_2C_2@C_2(230933)-C_{98} are the most stable isomers because of their thermodynamic and kinetic stabilities.

Chen *et al.* and Deng *et al.* discussed the possible geometric shapes of carbide clusters with different M–M distances,[43,44] and revealed that Sc_2C_2 was a planar, twisted unit. The structures of the most stable isomers of M_2C_2@C_{98} and M_2@C_{100} (M = La, Y, Sc) are shown in Fig. 2, and some of their structural parameters are listed in Table 2. For M_2C_2@C_{98} isomers, the Sc_2C_2 cluster tends to retain a linear structure, while La_2C_2 tends to form a butterfly-shaped structure. As shown in Table 2, the average La–C–C angle is about 83°, while that of Sc–C–C is about 162°, and the $d_{M\text{-cage}}$ values for La and Sc are 2.65 Å and 2.29 Å, respectively. They all have very similar C–C distances (~1.26 Å) in the cages, indicating the existence of a triple bond between the two carbon atoms, which is also consistent with the NBO bonding analysis (Table S8†). These results are very similar to the previous results of M_2C_2@C_{96} (M = La, Y, Sc) reported by Zheng *et al.*[34] On the other hand, the longest distances of the surfaces of three cages are 9.71, 9.70 and 9.69 Å, which are all very close to the corresponding value for the empty cage (9.71 Å), showing that the encapsulation of M_2C_2 has an insignificant effect on the shape of the cage. For M_2@C_{100} isomers, the $d_{M\text{–}M}$ values are much larger than those in M_2C_2@C_{98} isomers. The metal atoms are oriented with the longest metal–metal distances to minimize the electrostatic repulsion between them.

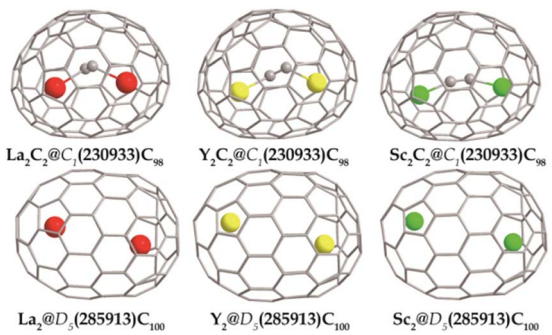

Fig. 2 Geometric structures of the most stable isomers of M_2@C_{100} and M_2C_2@C_{98} (M = La, Y, and Sc).

The calculated $d_{La\text{-cage}}$ and $d_{La\text{–}La}$ are 2.50 and 5.63 Å, respectively, which are very close to the experimentally reported values of 2.45 and 5.74 Å.[35] However, for Y and Sc, their $d_{M\text{-cage}}$ values decrease and $d_{M\text{–}M}$ values increase correspondingly, suggesting that the interactions between the Sc atoms and the nearby hexagons are the strongest, compared to the cases of Y and La. The longest distances between the two carbon atoms along the axis are 10.59 Å for La, 10.44 Å for Y and 10.43 Å for Sc, respectively. These distances are all much longer than that of the empty cage (10.28 Å), indicating that the cages are elongated after the metal clusters of M_2 are encapsulated.

NBO charge distributions of M_2C_2 or M_2 entrapped in cages C_1(230933)-C_{98} or D_5(285913)-C_{100} were employed and are shown in Fig. S2.† For all structures, carbon cages and encapsulated carbon atoms present negative charge states and metal atoms present positive charge states. The carbon atoms in carbide clusters are much more negatively charged than those on cages. It has also been found that the electrons are more centralized at the adjacent pentagon pole. The strong electronic interaction between the metal ion and the pentagon also helps to significantly stabilize the whole EMF.

In order to investigate the electronic structures of the thermodynamically favorable isomers, frontier molecular orbitals of M_2C_2@C_{98} and M_2@C_{100} (M = La, Y, Sc) are presented in Fig. 3. In M_2C_2@C_1(230933)-C_{98} isomers, all HOMO and LUMO orbitals have similar energy levels. The HOMO–LUMO gap of the C_1(230933)-C_{98} empty cage is enlarged when the cage encapsulates M_2C_2 clusters. In other words, entrapping M_2C_2 clusters can obviously make the C_1(230933)-C_{98} cage more stable, and the type of metal element is independent of electronic structures. Similar results have been found for the isomers of M_2@D_5(285913)-C_{100} (Fig. 3b). In these species, the HOMO is mainly localized on the carbon cage. However, the LUMO is completely localized on the two encaged metals. It shows a very unique situation in these isomers, in which the metal ions with 3+ oxidation state undergoing strongly repulsive Coulomb interaction might still have metallic interactions over a very long distance of 5–6 Å. The results also indicate that such structures might have a very stable and less reactive carbon cage.

These results can be compared with the previous results of M_2C_{98} (M = La, Y. Sc) reported by Zheng *et al.*[34] Table 3 shows the relative energies of the most stable isomers at 0 K. It is

Table 2 Structural parameters of M_2 or M_2C_2 clusters in some important M_2C_{100} species

	M–C–C angle (deg)	$d_{M\text{–}M}$[a] (Å)	$d_{C\text{–}C}$[b] (Å)	$d_{M\text{–}C}$[c] (Å)	$d_{M\text{–cage}}$[d] (Å)	L[e] (Å)
La_2C_2@C_1(230933)-C_{98}	84.4, 82.5	4.58	1.26	2.54, 2.55	2.65	9.71
Y_2C_2@C_1(230933)-C_{98}	108.2, 131.4	4.95	1.26	2.28, 2.30	2.47	9.70
Sc_2C_2@C_1(230933)-C_{98}	158.8, 164.2	5.32	1.25	2.14, 2.15	2.29	9.69
La_2@D_5(285913)-C_{100}	—	5.63	—	—	2.50	10.59
Y_2@D_5(285913)-C_{100}	—	6.05	—	—	2.34	10.44
Sc_2@D_5(285913)-C_{100}	—	6.41	—	—	2.18	10.43

[a] Distance between two metal atoms. [b] Distance between carbide atoms. [c] Distance between metal atoms and neighbouring carbon atoms of carbine fragment. [d] Distance between metal atoms and the nearest carbon atoms of the fullerene cage. [e] Maximum distance of two carbon atoms on the cage. Values of L for the empty cages of C_{98} and C_{100} are 9.71 Å and 10.28 Å, respectively.

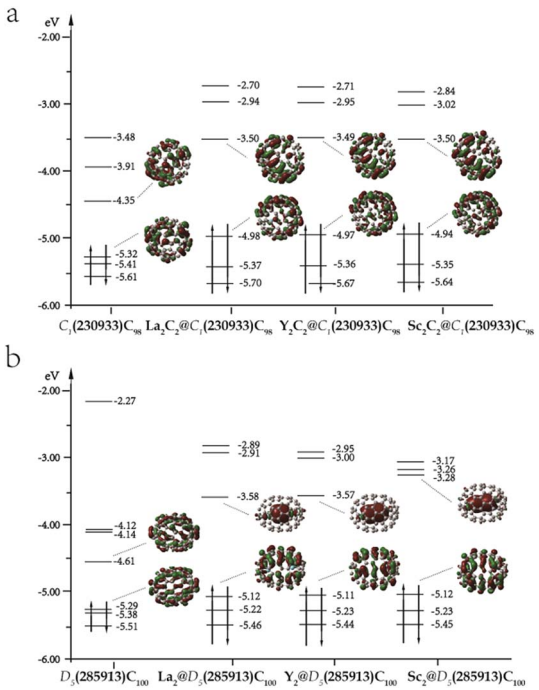

Fig. 3 Main frontier molecular orbitals of the most stable isomers of $M_2@C_{100}$ (bottom) and $M_2C_2@C_{98}$ (top) (M = La, Y, and Sc) and corresponding cages.

revealed that for M_2C_{98} and M_2C_{100} species, the classical dimetallofullerenes have a lower energy for La, but a higher energy for Sc. On the other hand, with the size of the carbon cage increasing, the advantage of the dimetallofullerene gradually increases. In order to make the results more reliable, the method of M06-2X/6-31G(d) ~ Lanl2dz[40–42] was also applied to the lowest-energy isomers of $M_2@C_{100}$ and $M_2C_2@C_{98}$ (Tables S6–S8†). Although the energy values are different, the tendency remains the same. However, considering the temperature effect on the distribution of all possible isomers, it should be noticed that the most stable species at higher temperatures, such as 3500 K, are still governed by metal-carbide EMFs, except in the case of La_2C_{100}. The result also implies that dimetallofullerenes might be more readily synthesized experimentally for carbon cages with larger sizes (n > 100). A systematic calculation on M_2C_{102} may help us to see if the suggestion is correct. The relevant work is ongoing in our lab.

Table 3 Comparison of the relative energies of the most stable isomers of M_2C_{100} and M_2C_{98} (M = La, Y, and Sc) at 0 K[a]

$M_2C_2@C_{2n-2}$	$M_2@C_{2n}$	ΔE^b
$La_2C_2@C_{96}$-191809	$La_2@C_{98}$-168785	−4.8
$Y_2C_2@C_{96}$-191809	$Y_2@C_{98}$-168785	17.1
$Sc_2C_2@C_{96}$-191809	$Sc_2@C_{98}$-230924	19.7
$La_2C_2@C_{98}$-230933	$La_2@C_{100}$-285913	−34.6
$Y_2C_2@C_{98}$-230933	$Y_2@C_{100}$-285913	−10.7
$Sc_2C_2@C_{98}$-230933	$Sc_2@C_{100}$-285913	−0.9

[a] Energies of M_2C_{98} species were taken directly from ref. 33. [b] Relative energies (in kcal mol^{-1}) were calculated by $\Delta E = E(M_2@C_{2n}) - E(M_2C_2@C_{2n-2})$.

Conclusions

Theoretical investigations have been performed on EMFs of M_2C_{100} (M = La, Y, Sc) by DFT calculation. In all cases, isomers of $M_2@D_5(285913)$-C_{100} are the lowest-energy species. However, statistical thermodynamic analysis shows that the most stable isomers under high temperatures (for example, T = 3000 K) should be metal-carbide endohedral fullerenes, except for La metal. Based on these results, the main product in electric arc experiments for La_2C_{100} should be $La_2@D_5(285913)$-C_{100}, which has been proven by the successful synthesis and X-ray crystallographic characterization conducted by Christine M. Beavers *et al.* in 2011.[29] For Sc_2C_{100}, the main products should be $Sc_2C_2@C_1(230933)$-C_{98}, and for Y_2C_{100}, the main products should be $Y_2C_2@C_1(230933)$-C_{98}, although some classical dimetallofullerenes might also be synthesized in the process. Further analysis on the geometric structures of $M_2C_2@C_{98}$ and $M_2@C_{100}$ showed that the positions of M_2 or M_2C_2 clusters rely very much on metal atoms. The effects of the encaged clusters on energies and shapes of the cages are also compared. Although both M_2 and M_2C_2 clusters can make outside cages more stable, the M_2C_2 clusters have a lesser effect on the shapes of the cages than M_2 clusters. The analyses on NBO charge distributions and frontier molecular orbitals reveal a strong electrostatic interaction between metal atoms and cages. It is also revealed that the LUMO orbital is mainly distributed on the metal atoms in the species of $M_2@C_{100}$. Simulated IR spectra of main M_2C_{100} isomers are shown in Fig. S4.† These results not only provide some valuable information for the experimental characterization and synthesis of large EMF species of M_2C_{100}, but can also help us to determine structures of larger EMFs of M_2C_{2n} ($2n$ > 100, M = La, Y, Sc).

Acknowledgements

Financial support from the National Natural Science Foundation of China (No. 21475065, 21627801) is gratefully acknowledged.

Notes and references

1 A. A. Popov, S. F. Yang and L. Dunsch, *Chem. Rev.*, 2013, **113**, 5989–6113.
2 X. Lu, L. Feng, T. Akasaka and S. Nagase, *Chem. Soc. Rev.*, 2012, **41**, 7723–7760.
3 H. Zheng, X. Zhao, W. W. Wang, T. Yang and S. Nagase, *J. Chem. Phys.*, 2012, **137**, 14308.
4 H. Kurihara, X. Lu, Y. Iiduka, N. Mizorogi, Z. Slanina, T. Tsuchiya, T. Akasaka and S. Nagase, *J. Am. Chem. Soc.*, 2011, **133**, 2382–2385.
5 X. Lu, K. Nakajima, Y. Iiduka, H. Nikawa, N. Mizorogi, Z. Slanina, T. Tsuchiya, S. Nagase and T. Akasaka, *J. Am. Chem. Soc.*, 2011, **133**, 19553.

6 X. Lu, K. Nakajima, Y. Iiduka, H. Nikawa, T. Tsuchiya, N. Mizorogi, Z. Slanina, S. Nagase and T. Akasaka, *Angew. Chem., Int. Ed.*, 2012, **51**, 5889.
7 B. Cao, M. Hasegawa, K. Okada, T. Tomiyama, T. Okazaki, K. Suenaga and H. Shinohara, *J. Am. Chem. Soc.*, 2001, **123**, 9679–9680.
8 H. Kurihara, X. Lu, Y. Iiduka, H. Nikawa, M. Hachiya, N. Mizorogi, Z. Slanina, T. Tsuchiya, S. Nagase and T. Akasaka, *Inorg. Chem.*, 2012, **51**, 746.
9 J. Zhang, T. Fuhrer, W. Fu, J. Ge, D. W. Bearden, J. L. Dallas, J. C. Duchamp, K. L. Walker, H. Champion, H. F. Azurmendi, K. Harich and H. C. Dorn, *J. Am. Chem. Soc.*, 2012, **134**, 8487–8493.
10 C. R. Wang, T. Kai, T. Tomiyama, T. Yoshida, Y. Kobayashi, E. Nishibori, M. Takata, M. Sakata and H. Shinohara, *Angew. Chem., Int. Ed.*, 2001, **40**, 397.
11 H. Kurihara, X. Lu, Y. Iiduka, H. Nikawa, N. Mizorogi, Z. Slanina, T. Tsuchiya, S. Nagase and T. Akasaka, *J. Am. Chem. Soc.*, 2012, **134**, 3139.
12 Y. Yamazaki, K. Nakajima, T. Wakahara, T. Tsuchiya, M. O. Ishitsuka, Y. Maeda, T. Akasaka, M. Waelchli, N. Mizorogi and H. Nagase, *Angew. Chem., Int. Ed. Engl.*, 2008, **47**, 7905.
13 T. Yumura, Y. Sato, K. Suenaga and S. Iijima, *J. Phys. Chem. B*, 2005, **109**, 20251.
14 Y. Iiduka, T. Wakahara, K. Nakajima, T. Nakahodo, T. Tsuchiya, Y. Maeda, T. Akasaka, K. Yoza, M. T. H. Liu, N. Mizorogi and S. Nagase, *Angew. Chem., Int. Ed.*, 2007, **46**, 5562.
15 Z. Q. Shi, X. Wu, C. R. Wang, X. Lu and H. Shinohara, *Angew. Chem., Int. Ed.*, 2006, **45**, 2107.
16 K. Tan and X. Lu, *Chem. Commun.*, 2005, 4444.
17 M. Krause, M. Hulman, H. Kuzmany, O. Dubay, G. Kresse, K. Vietze, G. Seifert, C. Wang and H. Shinohara, *Phys. Rev. Lett.*, 2004, **93**, 137403.
18 Y. Iiduka, T. Wakahara, K. Nakajima, T. Tsuchiya, T. Nakahodo, Y. Maeda, T. Akasaka, N. Mizorogi and S. Nagase, *Chem. Commun.*, 2006, 2057.
19 W. Cai, L. Bao, S. Zhao, Y. Xie, T. Akasaka and X. Lu, *J. Am. Chem. Soc.*, 2015, **137**, 10292.
20 W. Cai, F. Li, L. Bao, Y. Xie and X. Lu, *J. Am. Chem. Soc.*, 2016, **138**, 6670.
21 C. R. Wang, T. Kai, T. Tomiyama, T. Yoshida, Y. Kobayashi, E. Nishibori, M. Takata, M. Sakata and H. Shinohara, *Nature*, 2000, **408**, 426.
22 H. Kurihara, X. Lu, Y. Iiduka, N. Mizorogi, Z. Slanina, T. Tsuchiya, S. Nagase and T. Akasaka, *Chem. Commun.*, 2012, **48**, 1290.
23 T. Inoue, T. Tomiyama, T. Sugai, T. Okazaki, T. Suematsu, N. Fujii, H. Utsumi, K. Nojima and H. Shinohara, *J. Phys. Chem. B*, 2004, **108**, 7573.
24 H. Kato, A. Taninaka, T. Sugai and H. Shinohara, *J. Am. Chem. Soc.*, 2003, **125**, 7782.
25 B. P. Cao, T. Wakahara, T. Tsuchiya, M. Kondo, Y. Maeda, G. M. A. Rahman, T. Akasaka, K. Kobayashi, S. Nagase and K. Yamamoto, *J. Am. Chem. Soc.*, 2004, **126**, 9164.
26 T. Akasaka, S. Nagase, K. Kobayashi, M. Walchli, K. Yamamoto, H. Funasaka, M. Kako, T. Hoshino and T. Erata, *Angew. Chem., Int. Ed. Engl.*, 1997, **36**, 1643.
27 B. Q. Mercado, A. Jiang, H. Yang, Z. Wang, H. Jin, Z. Liu, M. M. Olmstead and A. L. Balch, *Angew. Chem., Int. Ed. Engl.*, 2009, **48**, 9114.
28 H. Yang, C. Lu, Z. Liu, H. Jin, Y. Che, M. M. Olmstead and A. L. Balch, *J. Am. Chem. Soc.*, 2008, **130**, 17296.
29 C. M. Beavers, H. Jin, H. Yang, Z. Wang, X. Wang, H. Ge, Z. Liu, B. Q. Mercado, M. M. Olmstead and A. L. Balch, *J. Am. Chem. Soc.*, 2011, **133**, 15338.
30 S. F. Yang and L. Dunsch, *Angew. Chem., Int. Ed.*, 2006, **45**, 1299.
31 T. Yang, X. Zhao and S. Nagase, *Phys. Chem. Chem. Phys.*, 2011, **13**, 5034.
32 A. A. Popov and L. Dunsch, *J. Am. Chem. Soc.*, 2007, **129**, 11835.
33 R. Valencia, A. Rodríguez-Fortea and J. M. Poblet, *J. Phys. Chem. A*, 2008, **112**, 4550.
34 H. Zheng, X. Zhao, W. W. Wang, J. S. Dang and S. Nagase, *J. Phys. Chem. C*, 2013, **117**, 25195.
35 X. Zhao, W. Y. Gao, T. Yang, J. J. Zheng, L. S. Li, L. He, R. J. Cao and S. Nagase, *Inorg. Chem.*, 2012, **51**, 2039.
36 Y. Guo, T. Yang, S. Nagase and X. Zhao, *Inorg. Chem.*, 2014, **53**, 2012.
37 M. J. Frisch, G. W. Trucks, H. B. Schlegel, G. E. Scuseria, M. A. Robb, J. R. Cheeseman, G. Scalmani, V. Barone, B. Mennucci, G. A. Petersson, H. Nakatsuji, M. Caricato, X. Li, H. P. Hratchian, A. F. Izmaylov, J. Bloino, G. Zheng, J. L. Sonnenberg, M. Hada, M. Ehara, K. Toyota, R. Fukuda, J. Hasegawa, M. Ishida, T. Nakajima, Y. Honda, O. Kitao, H. Nakai, T. Vreven, J. A. Montgomery Jr, J. E. Peralta, F. Ogliaro, M. Bearpark, J. J. Heyd, E. Brothers, K. N. Kudin, V. N. Staroverov, R. Kobayashi, J. Normand, K. Raghavachari, A. J. Rendell, C. Burant, S. S. Iyengar, J. Tomasi, M. Cossi, N. Rega, J. M. Millam, M. Klene, J. E. Knox, J. B. Cross, V. Bakken, C. Adamo, J. Jaramillo, R. Gomperts, R. E. Stratmann, O. Yazyev, A. J. Austin, R. Cammi, C. Pomelli, J. W. Ochterski, R. L. Martin, K. Morokuma, V. G. Zakrzewski, G. A. Voth, P. Salvador, J. J. Dannenberg, S. Dapprich, A. D. Daniels, O. Farkas, J. B. Foresman, J. V. Ortiz, J. Cioslowski and D. J. Fox, *Gaussian 09, Revision A.01*, Gaussian, Inc., Wallingford, CT, 2009.
38 Z. Slanina, *Int. Rev. Phys. Chem.*, 1987, **6**, 251.
39 A. Nicklass, M. Dolg, H. Stoll and H. Preuss, *J. Chem. Phys.*, 1995, **102**, 8942.
40 R. S. Zhao, Y. J. Guo, P. Zhao, M. Ehara, S. Nagase and X. Zhao, *J. Phys. Chem. C*, 2016, **120**, 1275–1283.
41 Y. Zhao and D. G. Truhlar, *Theor. Chem. Acc.*, 2008, **120**, 215–241.
42 A. Dreuw and M. Headgordon, *Chem. Rev.*, 2005, **105**, 4009–4037.
43 C. H. Chen, K. B. Ghiassi, M. R. Ceron, M. A. G. Ayala, L. Echegoyen, M. M. Olmstead and A. L. Balch, *J. Am. Chem. Soc.*, 2015, **137**, 10116.
44 Q. Deng and A. A. Popov, *J. Am. Chem. Soc.*, 2014, **136**, 4257.

